JOURNAL OF MATERIALS SCIENCE **34** (1999) 5927–5936

The effect of time and temperature on flexural creep and fatigue strength of a silica particle filled epoxy resin

M. K. McMURRAY, SHIGEO AMAGI
The First Department of Materials Research, Insulating Materials Group, Hitachi Research Laboratory, Hitachi, Ltd., Hitachi-shi, Japan 319-12

Composite materials that use an epoxy resin as a matrix resins have superior mechanical properties over standard structural materials, but these materials exhibit time and temperature behavior when used for long periods and under high temperatures. This time and temperature behavior has not been fully explained. The purpose of this paper is to further describe this time and temperature behavior, increasing the reliability of this class of composite materials. The time and temperature dependence of flexural strength was examined by creep and fatigue testing. Flexural creep tests were carried out at various temperatures below the glass transition temperature. Flexural fatigue tests were carried out at various stress ratios, temperatures below the glass transition temperature and 2 frequencies. The time-temperature superposition principle held for the flexural creep strength of this material. A method to predict flexural creep strength based on the static strength master curve and the cumulative damage law is proposed. When the fatigue frequency was decreased while temperature and stress ratio are held constant the flexural fatigue strength decreases. The time-temperature superposition principle was also found to hold for the flexural fatigue strength with respect to frequency.

1. Introduction

Epoxy resin with a filler, such as silica or alumina powder, because of its excellent electrical properties, small thermal expansion coefficient, strength and modulus, is being used in many electric products. For example, the composite tested in this paper is being used in molded transformers, the propulsion coils for the magnetic levitating vehicle and LSI encapsulation. In these applications the material undergoes complex loading, for example fatigue and creep loading. Propulsion coils and transformer applications require the composite to prevent the deflection of the windings of the coils due to magnetic forces. The material must also sustain its properties as the temperature increases during operation. It is commonly known that the mechanical behavior of epoxy resin, and composites made with these resins show viscoelastic behavior [1–6]. This viscoelastic behavior is a major concern when designing structures for adverse environmental conditions and long periods, such as the applications mentioned above. This report is the study of the influence of time and temperature on the failure strength behavior of this material subjected to complex loading.

Many papers have been written on the effect of filler in polymer composites on the mechanical properties [7–14]. Most of the papers like Brown and Kim *et al*., discuss the effect of filler on the modulus and toughness of the composite. Brown found that depending on the type of filler the modulus and toughness will increase with an increase in filler. This increase in filler usually lead to a decrease in static and impact strength. Kim *et al*. discovered that for less crosslinked epoxy resins, the fracture toughness increases as particle size decreases but size effects were not seen for highly crosslinked epoxy resins. The finding of no size effects was based on the finding that there was no change in the maximum shear deformation for varying particle size.

Static strength of a composite similar to the one used in this report was tested by Nishimura *et al*. [15]. They found that this composite's static strength decreased with temperature but did not examine the deflection rate effect. They also found that at low temperatures the initiation of fracture began in the silica particles. At high temperatures they explained that the major cause of failure was due to the interface between the particle and the resin. Creep strength of this material was also examined by Nishimura. They noticed that as temperature was increased the slope of the strain-time graphs increases. They also commented that the creep strength versus time curves were practically horizontal showing little slope. Comparison of creep and fatigue strength showed that at low temperatures the creep strength was higher than the fatigue strength.

Sinien *et al*. after performing creep tests on glass bead filled polyethylene believes that creep damage plays an important role at high stress levels [16]. Sinien showed

that the particles improved the creep resistance at low stresses but at high stress levels a low volume fraction of particles resulted in the neat resin creep resistance being higher than the filled composite. At low stress level changing the adhesive conditions at the interface of the particles and the matrix had little effect. At high stress and low adhesive properties the creep resistance equals that of the neat resin.

Fatigue properties of neat thermoset resins have been analyzed by several researchers [17, 18]. Barron *et al*. found that as temperature increases the crack growth rate decreases although the failure stress decreases. He also found that a rubber modifier helped decrease the crack growth rate. An increase in fatigue resistance was attributed to a decrease in the crack propagation rate, which can be achieved from the addition of a rubber modifier.

Fatigue testing of filled thermoset composites has mainly been concerned with the effect of the amount and shape of the filler used in these composites [7, 15, 19, 20]. Many papers report the influence on the amount of particulate filler and its effects on the strength of the composite. Brown concluded that the addition of a glass bead filler decreased the flexural strength of the composite when conducting strain controlled fatigue tests. Adhesion between the filler and matrix is believed to significantly influence the fatigue properties because of the stress concentrations around the fillers [7]. Nishimura *et al*. found that fatigue strength of a silica filled epoxy resin was dependent on the type of stress input wave and mean stress [15]. They also found that the silica filled epoxy resin's fatigue strength was independent of the frequency range tested (1–10 Hz). They concluded that most of the fracture results could be attributed to the brittle fracture of the particles.

Research on the fatigue stress ratio influence on the strength of epoxy matrix FRP (Fiber Reinforced Plastics) has been performed previously [21–24]. Results from Miyano *et al*. and others showed that FRP fatigue strength dependence on stress ratio changes as temperature increases to the glass transition temperature of the matrix resin. Fatigue strength was measured with several ratios of mean stress to stress amplitude ranging from near zero to 1. In comparison with the other stress ratios the lowest fatigue strength at room temperature occurred when stress ratio was near zero for a given time. When the temperature neared the glass transition temperature, the stress ratio of near zero had the highest strength for a given time. Satin woven FRP composites showed a smaller difference of strength due to stress ratio when compared to unidirectional FRP. This behavior was explained to originate from the matrix resin therefore this behavior should also appear in particle filled composites.

Another variable of fatigue testing that needs to be considered is frequency. Frequency effect from the point of view of hysteric heating on polymer composite was studied by Hertzberg *et al*. [25]. The authors described the effect due to frequency caused by heating and the associated loss of stiffness. By cooling the specimens with water they noticed a decrease in crack propagation of 2.5%. They also commented that the effect of frequency is dependent on the viscoelastic properties and geometry of the specimens. Broutman *et al*. also focused on the temperature rise due to frequency but included that stress level was also a factor [26]. He concluded that epoxy resins are cyclic dependent not time dependent.

The previous research clearly shows that problems can arise when using polymer matrix composite materials at high temperature or extended times. Some preliminary results have been published for this specific material [15, 27]. This paper will further explain the mechanical behavior of this material. Since it has been previously seen that the static strength shows viscoelastic behavior we assume that the creep and fatigue results discussed here will also.

2. Experimental procedure

2.1. Specimen preparation

Specimens were an epoxy resin with crystalline silica particle filler. The epoxy resin and crystalline silica particles were mixed and poured into molds made of steel plates coated with a mold release of silicon oil, to produce specimens approximately 5 mm thick. Air bubbles were removed by placing the molds in a vacuum. Curing temperature and time were 130 °C for 3 h then 150 °C for 5 h. These molds were then allowed to cool to 25 °C at a rate of 30 °C/h. The specimens for creep and fatigue testing were cut and sanded to dimensions of approximately $13 \times 5 \times 110$ mm (width, thickness, length). These specimens were after cured at a temperature of 170 °C for 5 h with a cool down rate of 30 °C/h. The silica content was 60% by volume with a maximum dimension of 80 μm and an average size of 7 μm, as given by the supplier.

2.2. Testing conditions

Flexural creep tests were performed in a 3-point bending jig at constant temperatures of 25, 40, 60, 80, and 100 °C. A creep testing machine (Orientic CP6-L-1000RX) with an attached constant temperature chamber was used to perform the creep tests. The span of the 3-point bending jig was 80 mm. At least three specimens were tested for each combination of stress and temperature.

Results for the flexural fatigue maximum stress versus number of cycles to failure curves were taken at a frequency of $f = 10$ and 0.1 Hz at constant temperatures of 60, 80, and 100 °C. Preliminary testing showed that at 10 Hz and 100 °C, the surface temperature of the specimen only increased 1, 2 °C, therefore we assume there was negligible effect from heating do to testing frequency. These tests were conducted with a computer controlled servopulser EHF-FD05-4LA (Shimadzu Co.) with an attached constant temperture chamber. Fatigue tests were performed under stress control and a sine input wave. At least three specimens were tested for each stress level in 3-point bending. Flexural fatigue was also conducted at several stress ratio R of 0.05, 0.5 and 0.8. Due to limitations of the fatigue testing machine's stroke, the span for fatigue test was changed to 60 mm.

2.3. Calculations

Three-point bending testing and calculations were performed according to the Japanese Industrial Standard (JIS) K 7203 [28]. Stress was calculated using Equation 1:

$$\sigma_{\max} = \frac{3P_b L}{2bh^2} \tag{1}$$

where $\sigma_{\max}$ is stress at failure (MPa), P_b is load at failure (N), L is the span (mm), b and h are the specimen width and thickness (mm), respectively [28]. Strain for creep tests $\varepsilon(t)$ was calculated using Equation 2:

$$\varepsilon(t) = \frac{6\delta(t)h}{L^2} \tag{2}$$

where $\delta(t)$ is the deflection (mm) at a given time t. Creep compliance was determined using the inverse of the modulus, giving the Equation 3:

$$Dc(t) = \frac{4bh^3\delta(t)}{PL^3} \tag{3}$$

where $Dc(t)$ is creep compliance (1/MPa) at a given time t, P is the constant load (N). Number of cycles were converted to time by the following Equation 4:

$$t = \frac{N}{f} \tag{4}$$

where t is time (s), N is number of cycles (cycles) and f is testing frequency (Hz). This allows the comparison of fatigue with other properties usually measured with time, as in static strength [22].

3. Results and discussion

3.1. Strain and compliance

Creep strains vs. log time for all five temperature and various stress levels are shown in Figs 1–3. The stress levels and the amount of strain is representative of all the data taken. There is nominal increase in strain before failure at 25 °C, but as temperature increase the amount of strain before failure increases. The largest amount of strain before failure occurs during $T = 100$ °C tests. It should also be pointed out that there is a relationship between applied stress and the amount of strain. The stress effect also increases with temperature. Even a difference due to stress can even be seen at 25 °C.

Fig. 4 is the compliance curves for all the temperature conditions and various stress levels. Again you can see, as in the strain data, that there is little change in compliance at $T = 25$ °C. As temperature increases, creep compliance also increases. As can be expected after considering the strain data, there is a stress influence on compliance, with higher stress levels the compliance of the composite increases. Even though it is thought that compliance for materials is constant for all stress levels this does not always hold true for viscoelastic materials. This means that with higher loads the modulus of the composite decreases, which is an important point for design applications.

3.2. Creep strength and compliance master curve

Flexural creep strength $\sigma(t)$ vs. log time t curves for all the testing temperatures are shown in Fig. 5. Flexural creep strength decreases with increasing temperature and time. Even though $T = 40$ °C data shows a slightly different slope than the other temperatures, it is believed with extended data the slope would be the same for all temperatures. There is also a more pronounced decrease in strength as temperature increases.

The master curves of flexural creep strength vs. reduced time t' at a reference temperature of $T_0 = 40$ °C is shown in Fig. 6. Construction of the master curve was accomplished by shifting the $\sigma(t)$ data points from Fig. 5. Flexural creep strength at the various temperatures were shifted along the log scale of time until the data points overlapped, creating a smooth curve. The time-temperature shift factor $a_{T_0}(T)$ is defined as:

$$a_{T_0} = \frac{t}{t'} \tag{5}$$

where t is the experimental time data, and t' is the reduced time. Since a smooth curve is produced when shifting the $\sigma(t)$ data with respect to time, the time-temperature superposition principle is applicable.

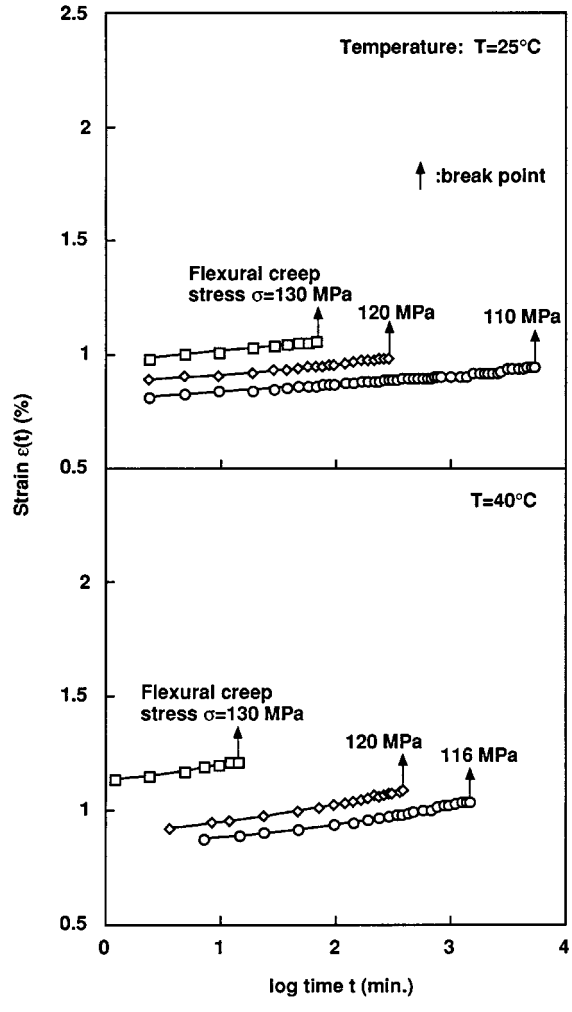

Figure 1 Flexural creep strain $\varepsilon(t)$ vs. time for $T = 25$ °C and 40 °C at various stress levels.

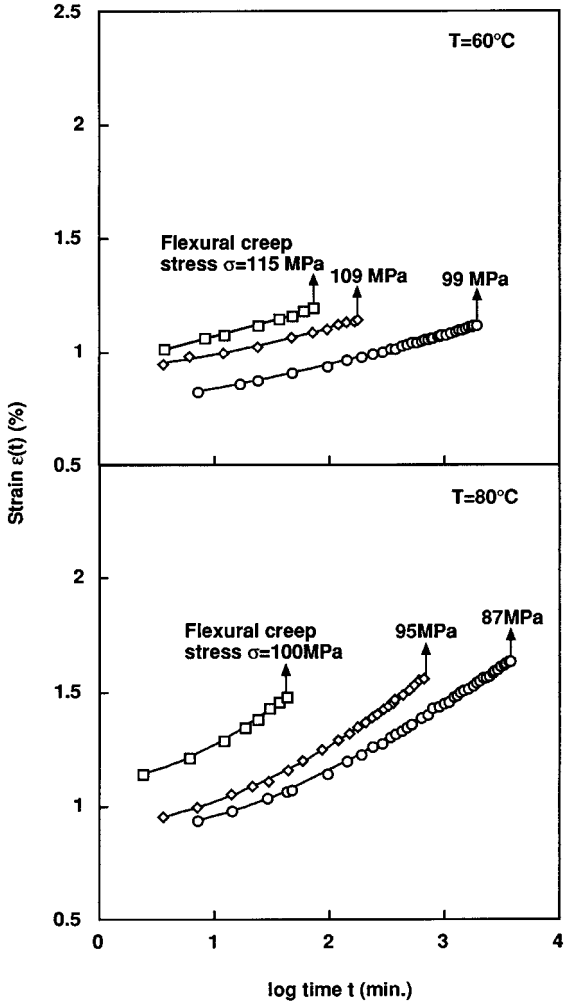

Figure 2 Flexural creep strain $\varepsilon(t)$ vs. time for $T = 60\,^{\circ}$C and $80\,^{\circ}$C at various stress levels.

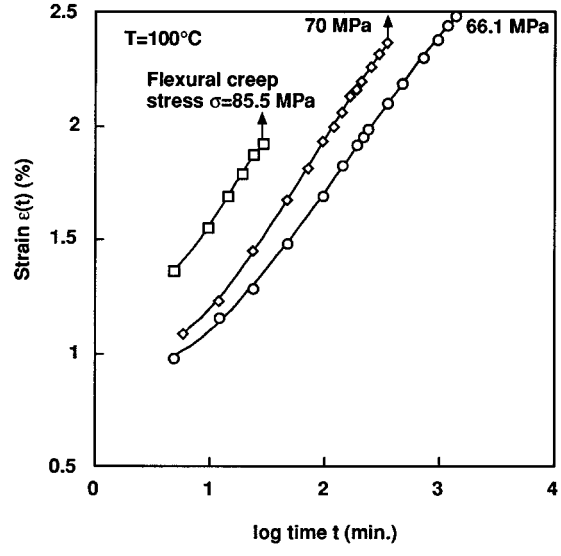

Figure 3 Flexural creep strain $\varepsilon(t)$ vs. time for $T = 100\,^{\circ}$C at various stress levels.

Flexural creep compliance master curves were produced in the same manner as the creep strength master curve, shown in Fig. 7a,b. The top master curve, Fig. 7a, is for a flexural creep stress level of $\sigma = 90$ MPa while the lower master curve, Fig. 7b, is for $\sigma = 110$ MPa. The experimental data shown in the left-hand side of the figure are an average of several data points. In the case when the stress range at that particular temperature was not conducted, the point was estimated by linear interpolation. The time-temperature superposition principle also holds for the flexural creep compliance for the composite material since smooth curves were produced. Two stress levels are shown because in previous graphs it was obvious that there is a compliance dependence on stress level. The time-temperature superposition principle held for both conditions, even thought both the stress and strain levels were different.

Fig. 8 shows the flexural creep strength and compliance master curve's time-temperature shift factors a_{T_0} vs. inverse of temperature T, and for the static strength and storage modulus from the matrix resin [10]. The time-temperature shift factors a_{T_0} changes drastically with temperature near the T_g of the matrix resin. Shift factors a_{T_0} are in good qualitative agreement with the solid lines, which represent Arrhenuis' equation. Therefore a_{T_0} can be represented by using activation energy ΔH and the Arrhenuis' Equation 6:

$$\log a_{T_0}(T) = \frac{\Delta H}{2.303R}\left[\frac{1}{T} - \frac{1}{T_0}\right] \qquad (6)$$

where ΔH is the activation energy (kJ mol^{-1}), R = gas constant (8.314×10^{-3} kJ K^{-1} mol^{-1}), T is the testing temperature (K) and T_0 is the reference temperature (K) [29, 30]. The static strength a_{T_0} can be assumed to agree well with Arrhenuis' equation, the neat resins modulus and static strength a_{T_0} until temperature near the T_g of the matrix resin. The modulus and static results were reported previously in Reference [27]. It has been shown that this composite becomes much more viscoelastic near the T_g of the neat resin.

The composite's time-temperature behavior is heavily influenced by the matrix resin. This can be concluded from the agreement between the storage modulus behavior of the matrix resin and the results of the master curves. The flexural creep compliance master curve's time-temperature shift factors do not correlate as well with the neat resin shift factors as do the flexural static strength data. This is because storage modulus and static strength testing were conducted under small strain ε conditions, but creep experiments were conducted at large strain ε level. It is believed that the time-temperature shift factors from a master curve of constant strain properties conducted under small strain (ex. relaxation modulus), would agree more closely with the neat resins storage modulus data.

3.3. Creep strength prediction

The prediction method of flexural creep strength is proposed based on the static strength master curve and the linear cumulative damage law [31]. Additionally, flexural creep tests should be carried out for several stress levels and temperatures to qualify the use of this prediction procedure.

Let $t_s(\sigma)$ and $t_c(\sigma)$ be the static and creep failure time for the stress σ. Further, suppose that the material experiences a stress history $\sigma(t)$ for $0 < t < t^*$ where t^* is the failure time under the stress history. The linear

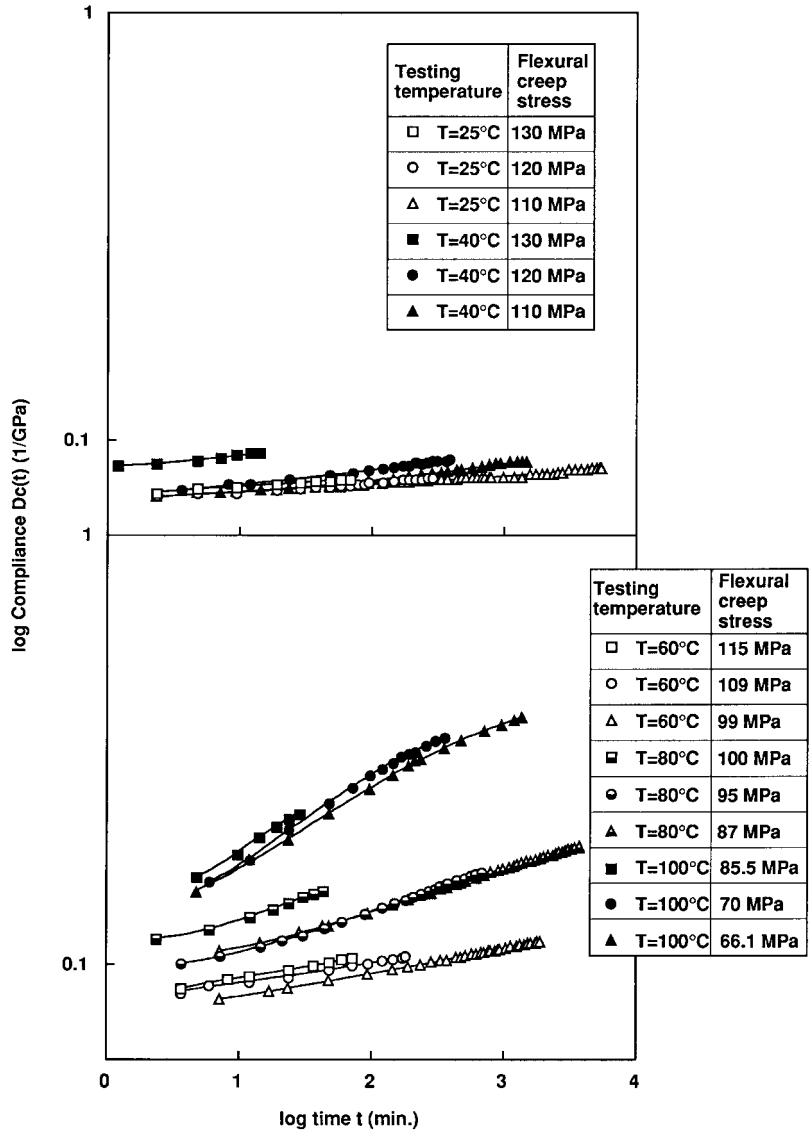

Figure 4 Flexural creep compliance $Dc(t)$ for all temperatures and various stress levels.

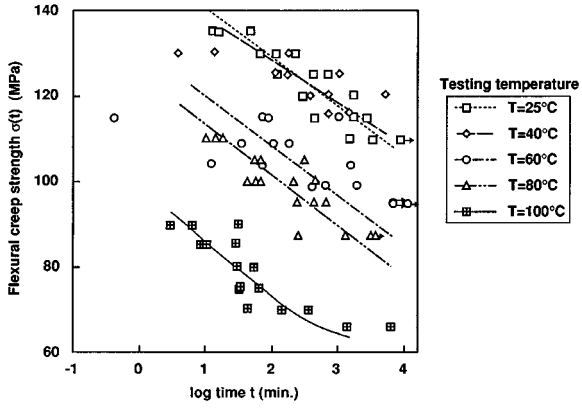

Figure 5 Flexural creep stress σ vs. time at various temperatures.

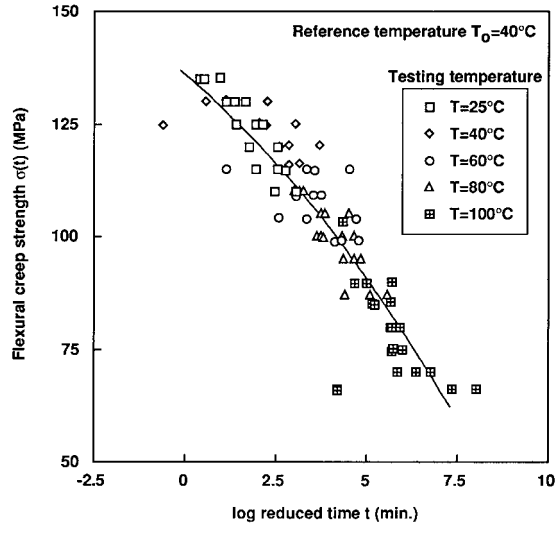

Figure 6 Flexural creep strength master curve.

cumulative damage law is:

$$\int_0^{t^*} \frac{dt}{t_c[\sigma(t)]} = 1. \qquad (6)$$

Our objective is to find the creep failure time $t_c(\sigma)$ from the static failure time $t_s(\sigma)$ and the linear cumulative damage law Equation 6.

Choose an increasing sequence of stress, σ_i ($i = 1, 2, 3, \ldots$), and denote the associated static and creep failure time by $t_s^{(i)}$ and $t_c^{(i)}$ as explained in Fig. 9. In the static test, the deflection rate is kept constant and

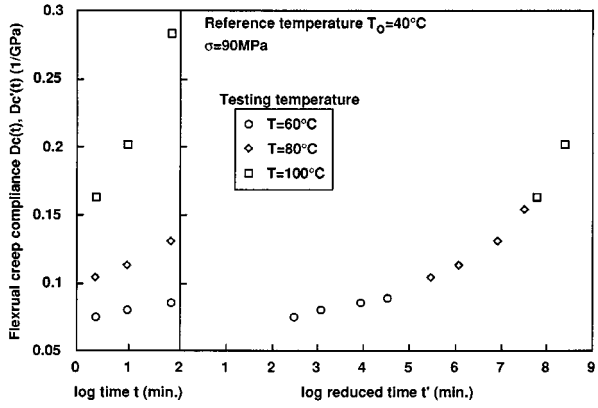

(a)

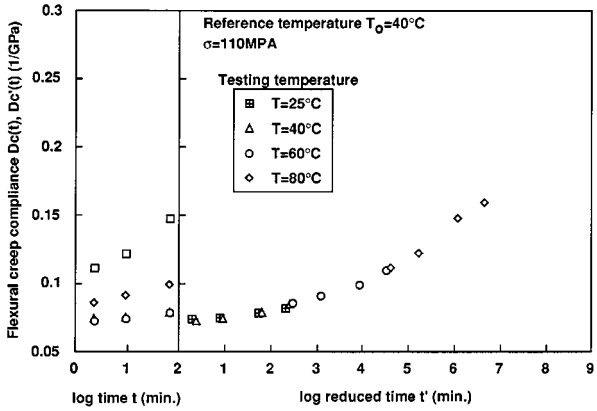

(b)

Figure 7 Master curves of flexural creep compliance for a reference temperature $T = 40\,^{\circ}\mathrm{C}$ and $\sigma = 90$, 110 MPa: (a) Flexural creep compliance master curve for $T_0 = 40\,^{\circ}\mathrm{C}$, $\sigma = 90$ MPa; (b) Flexural creep compliance master curve for $T_0 = 40\,^{\circ}\mathrm{C}$, $\sigma = 110$ MPa.

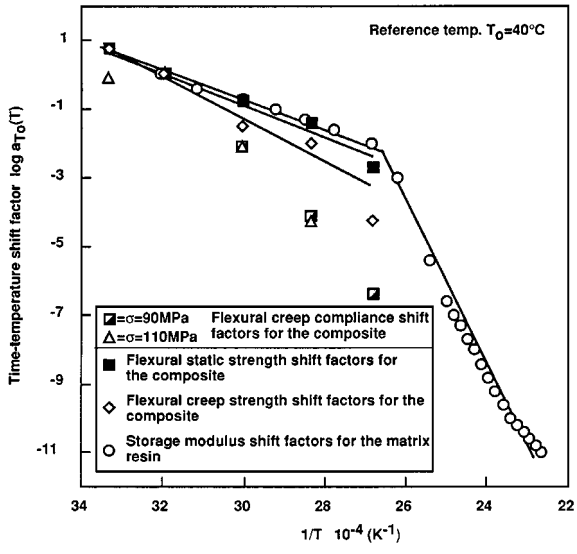

Figure 8 Time-temperature shift factors for flexural static and creep strength, flexural creep compliance and storage modulus for the matrix resin.

the force-deflection curves are assumed to be linear up to just before failure. It is therefore assumed, that the stress increases linearly during the static test. Further, it is assumed that the linear stress history can be approximate by a staircase function with steps $\sigma_1, \sigma_3, \sigma_5, \ldots$. Thus, the linear stress history up to the stress level σ_4 is replaced by σ_1 for $0 < \sigma < \sigma_2$ and σ_3 for $\sigma_2 < \sigma < \sigma_4$ (Fig. 9). By the aid of the linear cumulative damage

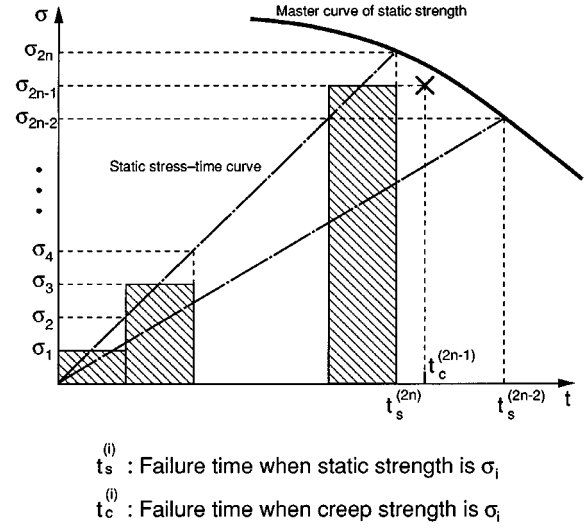

Figure 9 Explanation of creep prediction method.

law, the creep failure time $t_c^{(2n-1)}$ $(n = 1, 2, 3, \ldots)$ is expressed successively by as follows:

$$t_c^{(1)} = t_s^{(2)}$$

$$t_c^{(2n-1)} = \frac{t_s^{(2n)} t_s^{(2n-2)}}{n t_s^{(2n-2)} - (n-1) t_s^{(2n)}} \qquad (7)$$

Therefore the creep strength is evaluated from Equation 7 and the master curve of static strength in which the curve is extrapolated by a decaying exponential curve. First the master curve of static strength is curve fitted, usually with a 2 or 3 power equation to obtain static failure stress as a function of time. Then using this equation, static failure time is calculated for equal intervals of stress from low to high values within the experimental data range. These stress values now become the predicted creep stress values. Then using Equation 7 and the time calculated from the static master curve equation the creep failure time is calculated [32].

Fig. 10 is the prediction curve of flexural creep strength based on the cumulative damage law and the

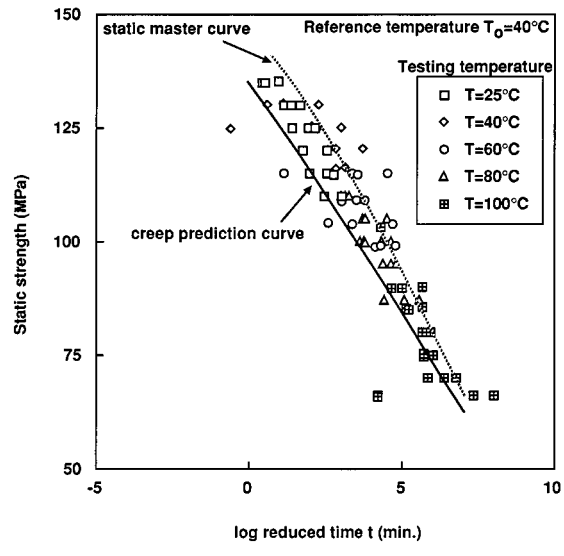

Figure 10 Flexural creep strength prediction curve.

static master curve. The solid line represents the prediction method. It is a conservative estimate of the flexural creep strength. This method would serve well during design when a conservative estimate creates a larger margin of safety. It seems that if an average was taken of the static master curve and this prediction method a more accurate estimate would be produced. We are hesitate to propose this because of no physical meaning behind using an average.

3.4. Explanation of stress ratio

Fatigue tests were conducted at 3 stress ratios, $R = 0.05$, 0.5 and 0.8. Stress ratio R is the ratio of minimum stress to maximum stress:

$$R = \frac{\sigma_{\min}}{\sigma_{\max}} \tag{7}$$

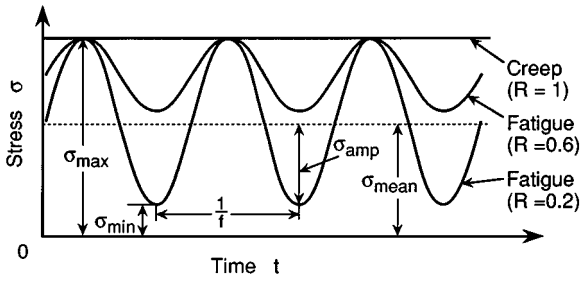

Figure 11 Explanation of stress ratio R.

where $\sigma_{\min}$ is the minimum stress and $\sigma_{\max}$ is the maximum stress during fatigue testing. Minimum stress $\sigma_{\min}$ is the smallest stress value during one fatigue cycle (1/frequency). Maximum stress $\sigma_{\max}$ is the largest stress value during one fatigue cycle. Mean stress σ_{mean} is the average value between $\sigma_{\min}$ and $\sigma_{\max}$, these definitions are explained graphically in Fig. 11. As R increases from 0 to 1 for a constant maximum stress, the stress amplitude goes to 0 and mean stress becomes equal to maximum stress. When R is small, this means that the stress amplitude is quite large in comparison with a large R, which has a small stress amplitude. This means that as R increases to 1 the stress amplitude becomes smaller but the mean stress becomes larger. Therefore damage due to creep loading should increase for large R values. This is shown in Fig. 11. Stress ratio of $R = 0.05$ is assumed to be equal to $R = 0$ since it is difficult to test at a smaller stress ratio with a 3 point bending jig. This is due to the loading point losing contact with the specimen creating an impact type condition. To obtain a range of values, specimens were also tested at stress ratios of $R = 0.5$ and $R = 0.8$.

3.5. Flexural fatigue strength

Flexural fatigue strength σ for all testing temperature and stress ratios are plotted in Fig. 12. Flexural fatigue strength σ is assumed to be equal to flexural

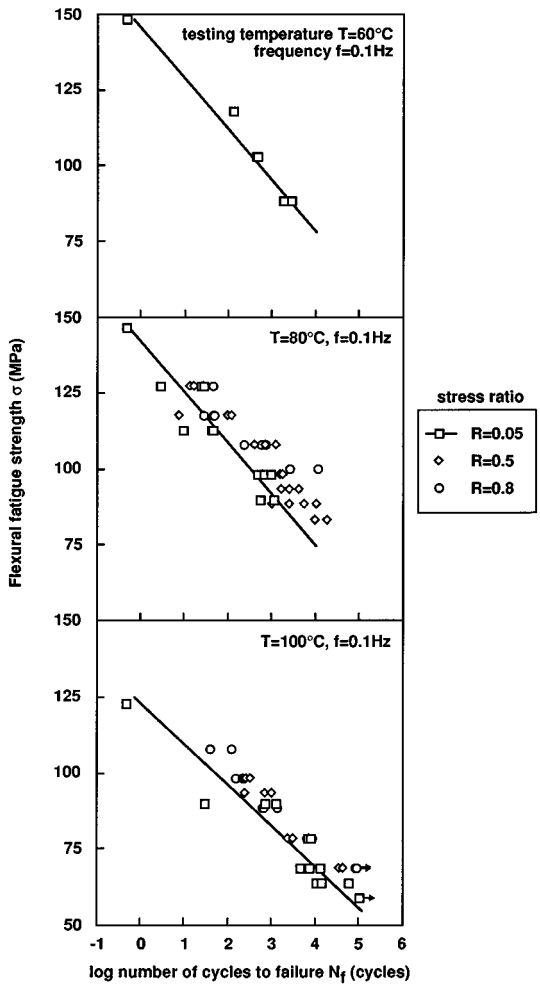

Figure 12 Flexural fatigue strength vs. log number of cycles to failure for various stress ratios R at constant temperatures.

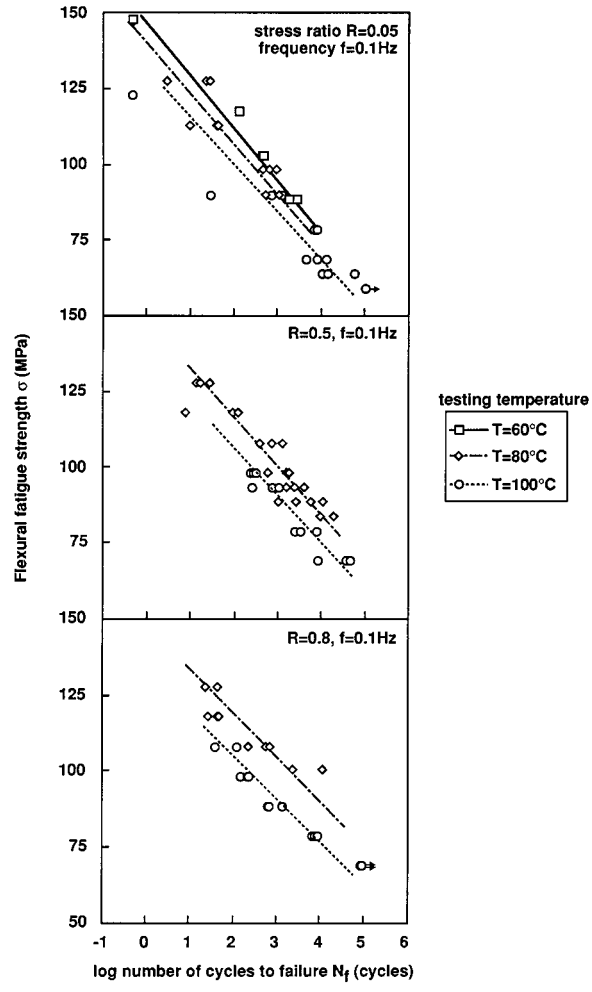

Figure 13 Flexural fatigue strength vs. number of cycles to failure for various temperature for each stress ratio R.

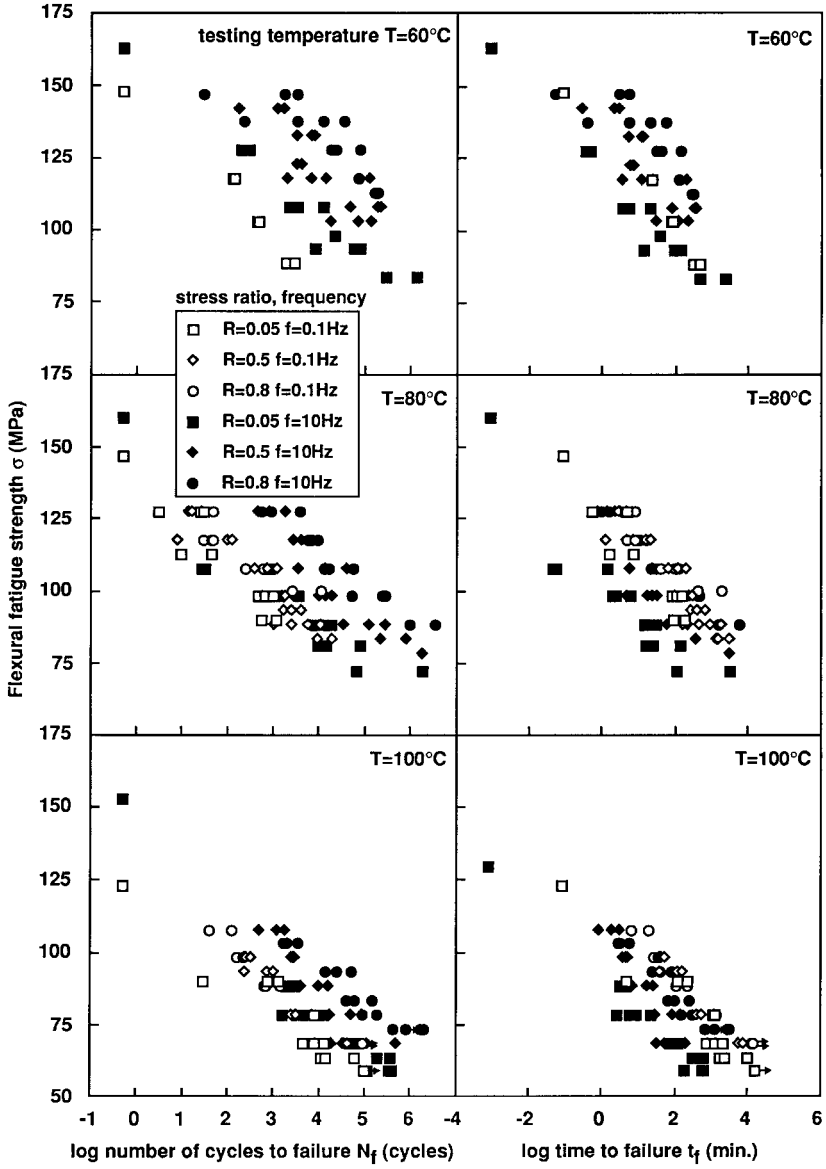

Figure 14 Flexural fatigue strength vs. number of cycles and time to failure for the 2 frequencies data.

static strength with a time to failure equal to $1/2$ cycle. The points at a log number to failure $N_f = -0.3$ and a stress ratio $R = 0.05$ for each temperature is flexural static results. Since static tests could not be conducted at log time to failure equal to -1.08 (calculated using Equation 4), stress values were arrived at by using the time-temperature superposition principle and the master curve of static strength [27]. Using the time-temperature shift factors from the modulus data of the matrix resin, the strength at log time to failure $t_f = -1.08$ was calculated.

As temperature increases, the difference in σ among the 3 stress ratios decreases, showing that as temperature increases, stress ratio has less of an influence on fatigue strength. The slopes of the curves for $R = 0.05$ and 0.8 are almost constant for all temperatures. From the data shown and previous results [27], at low temperatures the composite fails with little deformation but as the temperature increases the composite becomes more ductile and creep damage occurs.

The points at $N_f = -0.3$, static strength, corresponds well with the curves that represent fatigue strength at $R = 0.05$ for each temperature. This means, initial fatigue damage can be thought of a step-wise accumulation of damage equal to static strength at the same temperature with a time to failure equal to the time of $1/2$ fatigue cycle. Since the time-temperature superposition principle, using the time-temperature shift factors from the matrix resin, held for the static strength which corresponds well with the curves representing the fatigue strength, then it can also be said that the time-temperature superposition principle also holds for the initial fatigue strength.

A single stress ratio condition for each temperatures is plotted in Fig. 13. This shows clearly that the slope of the curves of all stress ratios changes little with temperature. The decrease in strength due to temperature becomes larger as stress ratio increases, this shows that creep damage increases with temperature and is an influence on fatigue strength.

3.6. Frequency influence

Fig. 14 shows flexural fatigue strength σ for all testing temperatures and stress ratios for frequencies $f = 0.1$ and 10 Hz. The left hand side is σ vs. log number of

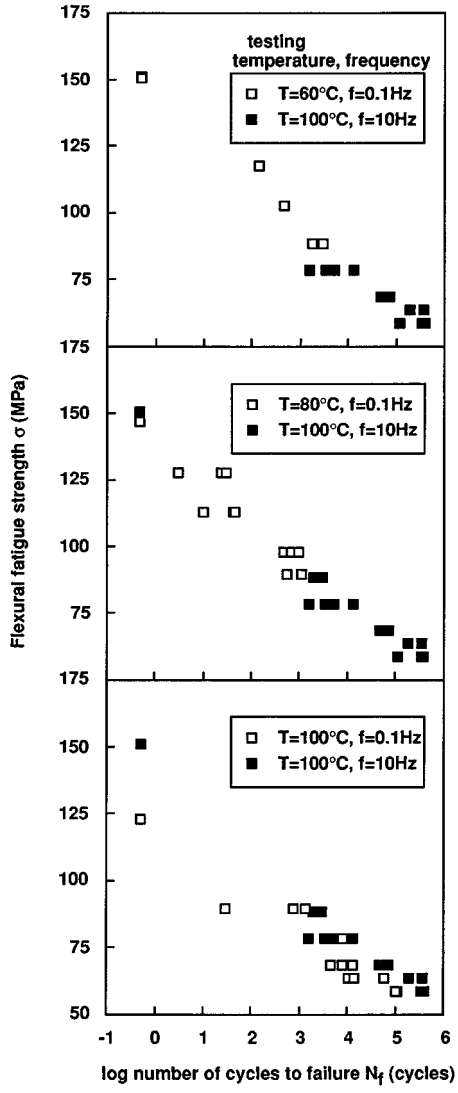

Figure 15 Flexural fatigue strength vs. number of cycles and time to failure for $R = 0.05$ and various temperatures and frequencies.

cycles to failure N_f while the right hand side is σ vs. log time to failure t_f. Equation 3 was used to convert number of cycles to failure to time to failure so that static strength results could be compared with fatigue strength results. One point that is noticed in both sides of the graph is that the scatter is reduced when testing frequency is decreased. From the N_f section of the figure it is seen that as temperature increases the effect of frequency lessens. When comparing the 2 frequencies, for a given number of cycles to failure N_f, $f = 10$ Hz test operate for less time than $f = 0.1$ Hz. In other words, since the frequency effect shown in N_f graphs decreases, time becomes less of a factor as temperature increases. For the same time to failure t_f, $f = 10$ Hz cycles more than $f = 0.1$ Hz. Therefore the t_f side shows that number of cycles effect is becoming stronger since $f = 10$ Hz data has a lower fatigue strength for a given time to failure t_f.

3.7. Application of the time-temperature superposition principle

We have shown that the time-temperature superposition principle holds for the initial flexural fatigue strength. To prove that this can be extended and applied to a change in frequency we again used the time-temperature shift factors $a_{T_0}(T)$ from the matrix resin's modulus data. The equation for time-temperature shift factor $a_{T_0}(T)$ (Equation 5) as applied to frequency is defined as:

$$a_{T_0} = \frac{t}{t'} = \frac{f'}{f} \tag{8}$$

where t is the experimental time data, t' is the reduced time, f is the testing frequency, and f' is the reduced frequency. Using Equation 8, $a_{T_0}(T)$ vs. $1/T$ curve (Fig. 8) from the static strength master curve, testing frequency of $f = 10$ Hz, and a $f' = 0.1$ Hz the testing temperature was calculated to be $T = 60\,^{\circ}$C.

Fig. 15 shows flexural fatigue strength σ vs. number of cycles to failure N_f for several temperatures. The graph clearly shown that the data from $T = 60\,^{\circ}$C, $f = 0.1$ Hz and $T = 100\,^{\circ}$C, $f = 10$ Hz overlap each other. As temperature increases the alignment of the 2 testing conditions lessens as is explained by the time-temperature superposition principle. If we had tested at temperatures below $T = 60\,^{\circ}$C, the $f = 0.1$ Hz data would have an increasing higher flexural fatigue strength.

This proves that the time-temperature also holds for the frequency behavior of flexural fatigue strength. This means that short time, high temperature tests results can be used to predict long term low temperature behavior.

4. Conclusions

The following conclusions were obtained from flexural creep and fatigue tests conducted at several temperatures and loading conditions for an epoxy resin containing a crystalline silica particle filler:

(1) The flexural creep strain and compliance is time, temperature and stress level dependent, becoming more viscoelastic near the glass transition temperature of the matrix resin.

(2) The flexural creep strength of the composite is time and temperature dependent. Even though the composite is viscoelastic in nature the slope of the flexural creep strength stress vs. time curves can be considered equal.

(3) The time-temperature superposition principle held for the flexural creep compliance and strength for this composite material.

(4) Using the static strength master curve and the cumulative damage law a conservative method was proved to be able to predict the flexural creep strength.

(5) The fatigue strength is time and temperature dependent, becoming more viscoelastic near the glass transition temperature of the matrix resin. The time-temperature superposition principle using the matrix resin's shift factors held for the initial fatigue strength behavior of the composite material.

(6) As temperature and stress ratio increased the fatigue strength also becomes more creep damage dependent.

(7) As temperature and frequency increase, number of cycles becomes more of an influence on fatigue strength than time.

(8) The time-temperature superposition principle using the time-temperature shift factors from the matrix resin's modulus master curve also holds for the frequency behavior. Since this principle holds true short time, high temperature tests results can be used to predict long term low temperature behavior.

References

1. Y. MIYANO, M. KANEMITSU, T. KUNIO and H. KUHN, *Journal of Composite Materials* **20** (1986) 520.
2. L. E. NIELSEN, "Mechanical Properties of Polymers" (Reinhold Publishing Corporation, New York, NY, 1962).
3. A. J. BARKER and H. VANGERKO, *Composites* **14**(2) (1983) 141.
4. K. PANNKOKE and H.-J. WAGNER, *Cryogenics* **31** (1991) 248.
5. Y. SADKIN and J. ABOUDI, *Composite Science and Technology* **36** (1989) 351.
6. M. G. NORTHOLT, *Journal of Material Science* **16** (1981) 2025.
7. S. K. BROWN, *The British Polymer Journal* **14** (1982) 1.
8. M. MIWA, A. TAKENO, K. HARA and A. WATANABE, *Composites* **26** (1995) 371.
9. A. C. MOLONEY, H. H. KAUSCH, T. KAISER and H. R. BEER, *Journal of Material Science* **22** (1987) 381.
10. A. G. EVANS, S. WILLIAMS and P. W. R. BEAUMONT, *ibid.* **20** (1985) 3668.
11. H. R. BEER and T. KAISER, *Fillers* (1986) 16.1–16.4.
12. G. TSAGAROPOULOS and A. EISENBERG, *Macromolecules* **28** (1995) 6067.
13. W. JIANG, H. LIANG, J. ZHANG, D. HE and B. JIANG, *Journal of Applied Polymer Science* **58**(3) (1995) 537.
14. D. S. KIM, K. CHO, J. K. KIM and C. E. PARK, *Polymer Engineering and Science* **36**(6) (1996) 755.
15. A. NISHIMURA, A. YAGUCHI and S. KAWAI, *Zairyou* **38**(434) (1989) 92, Japanese.
16. L. SINIEN, Z. ZIAOGUANG, Q. ZHONGNENG and Z. HAUN, *Journal of Materials Science Letters* **14** (1995) 1458.
17. K. HIGASHIBATA, T. MIYAMOTO, K. HAYASHI and T. TANAKA, *IEEE Japan* **114-B**(5) (1994) 539, Japanese.
18. D. L. BARRON, D. H. KELLEY and L. T. BLANKENSHIP, in Proceedings of 44th Annual Conference (Composite Institute, The Society of the Plastics Industry, Inc., 1989) p. 14-C-1.
19. A. YAGUCHI and A. NISHIMURA, *Zairyou* **42**(472) (1993) 40, Japanese.
20. S. W. SHANG, J. W. WILLIAMS and K-J. M. SÖDEHOLM, *Journal of Material Science* **30** (1995) 4323.
21. Y. MIYANO, M. K. MCMURRAY, J. ENYAMA and M. NAKADA, *Journal of Composite Materials* **28**(13) (1994) 1250.
22. M. K. MCMURRAY, M. NAKADA and Y. MIYANO, *ibid.* **29**(14) (1995) 1808.
23. *Idim.*, in Proceeding 40th International SAMPE Symposium and Exhibition (1995) 1316.
24. B. HARRIS, H. REITER, T. ADAM, R. F. DICKSON and G. FERNANDO, *Composites* **21**(3) (1990) 232.
25. R. W. HERZBERG and J. A. MANSON, *Fatigue Environ Temp Eff* (1993) 231.
26. L. J. BROUTMAN and S. K. GAGGAR, in Proceedings 27th Annual Technical Conference (Reinforced Plastics/Composites Institute, The Society of the Plastics Industry, Inc., 1972).
27. M. K. MCMURRAY and S. AMAGI, in Proceedings of 28th International SAMPE Technical Conference (1996) 699.
28. JIS, *Japanese Standards Association* **K 7203-1982** (1982).
29. F. SCHWARZL and A. J. STAVERMAN, *Journal of Applied Physics* **23**(8) (1952) 838.
30. M. L. WILLIAMS, R. F. LANDEL and J. D. FERRY, *Journal of the American Chemical Society* **77** (1955) 3701.
31. E. KREYSZIS, "Advanced Engineering Mathematics," 3rd ed. (John Wiley and Sons, Inc., New York, 1972) p. 723.
32. Y. MIYANO, M. K. MCMURRAY and R. MUKI, in Proceedings of 1995 ASME Summer Mechanics Conference (AMD-Vol. 204 Numerical Methods in Structural Mechanics 1995) 69.

Received 25 March 1997
and accepted 2 June 1999